# Bioactivation of New Harmonic Titanium Alloy to Improve and Control Cellular Response and Differentiation

André Rangel, Mylan Lam, Azziz Hocini, Vincent Humblot, Kei Ameyama, Véronique Migonney, Guy-François Dirras, Céline Falentin-Daudré

**Bioactivation of New Harmonic Titanium Alloy to Improve and Control Cellular Response and differentiation**

A. RANGEL[a], A.HOCINI[b], V. HUMBLOT[c,d], K. AMEYAMA[e], V. MIGONNEY[a], G. DIRRAS[b], C. FALENTIN-DAUDRE[a,*]

[a] Université Sorbonne Paris Nord, Institut Galilée, LBPS/CSPBAT, CNRS UMR 7244 , Villetaneuse, France
[b] Université Sorbonne Paris Nord, Institut Galilée, LSPM, CNRS UPR 3407 , Villetaneuse, France
[c] Sorbonne Université, Laboratoire de Réactivité de Surface (LRS), CNRS UMR 7197, Paris, F-75005, France
[e] Ritsumeikan University, College of Science and Engineering, Department of Mechanical Engineering, 1-1-1 Noji-Higashi, Kusatsu-city, Shiga 525-8577, Japan
[d] FEMTO-ST Institute, Université Bourgogne Franche-Comté, UMR CNRS 6174, 15B avenue des Montboucons, 25030 Besançon Cedex, France

* Corresponding author: falentin-daudre@univ-paris13.fr

## Graphical abstract

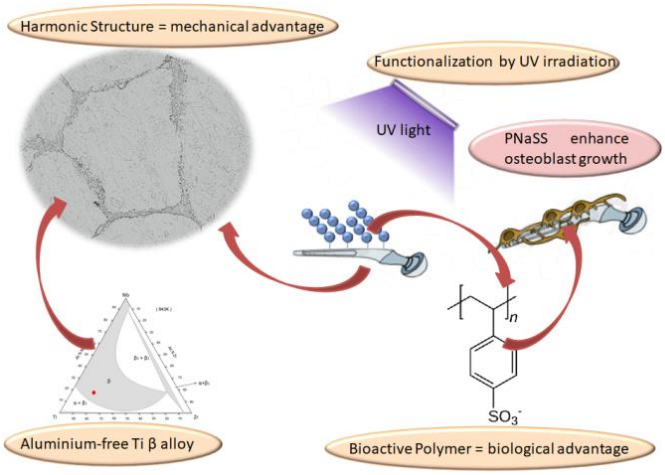

**Abstract**

*Objective* The purpose of this research article is to present the functionalization of a new titanium alloy of the system TiNbZr, by covalent grafting of a bioactive polymer (poly(sodium styrene sulfonate), PNaSS) using the "grafting from" technique to improve the biological response.

*Material and Method* Colorimetric assay, Fourier-transform infrared spectra recorded in attenuated total reflection mode (ATR-FTIR), Scanning electron microscopy (SEM), X-ray photoelectron spectroscopy (XPS), and water contact angle measurements (WCA) were applied to characterize the surfaces. The effect of the grafting on the biological response was assessed using MC3T3-E1 pre-osteoblast cells line.

*Results* This study has shown that our rates of grafting obtained on these new alloys are as good as (around 4,5 µg/cm$^2$) as those of grafting on classical alloys. In parallel, *in vitro* biological response study was carried out to assess toxicity, cell viability, and morphology on the titanium alloys TiNbZr functionalized. Moreover, results showed superior alkaline phosphatase activity and higher calcium deposition on grafted samples, implying a beneficial effect of the PNaSS in osteoinduction activity.

*Conclusions* Grafted TiNbZr improve the cell response in particular the oseointegration.

**Keywords:** titanium alloys, TiNbZr, polymers grafting, bioactive, UV irradiation, cell culture

## 1. Introduction

Titanium implants and their alloys represent a considerable share of the more than 1 million total hip implants and 5 million dental implants performed each year worldwide [1,2]. These materials have been used as implantable metals since the 1960s, largely due to their low density, desirable mechanical properties, and good surface stability granted by their high corrosion resistance [3]. Nevertheless, after they raised in popularity in the 1980s the advancement of biomaterials science showed that improvements should be made in both volume and surface properties to ensure a higher success rate for these implants. The first moves in this direction were the development of new titanium alloys, mainly beta phase, using non-

cytotoxic alloy elements [4]. The primary objective would be to bring the mechanical properties close to the values found in the bone, to prevent the mismatch when subjected to mechanical stress and consequent bone resorption due to the stress shielding effect [5], without risks to the patient even in the long term. This trend popularized titanium alloys containing Nickel, Molybdenum, Tantalum, and lately Niobium and Zirconium.

Alloys belonging to this ternary system achieved relative success between researchers for combining the beta phase stabilization of the Nb and the hardening effect of the solid solution by the presence of Zr [6]. Moving forward on this plan, our group recently used an innovative route to produce TiNbZr alloys using powder metallurgy, aiming to improve material strength without harming ductility. Through this methodology, alloys were produced with the so-called harmonic structure, composed of two distinct regions: a core of large grains surrounded by an ultra-fine particle shell [7-9]. This structure is expected to improve the yield stress due to grain boundary strengthening of the shell while keeping the ductility of the core, which has been previously confirmed in pure titanium [10-11].

Despite all the advantages in the bulk of the alloys, this process has a very limited impact on the surface's properties. Even if titanium alloys present fair osteointegration rates it is widely known that this process leans heavily on the surface characteristics such as wettability, topography, and chemical composition [12]. Thus, surface modifications and functionalization treatments could have a beneficial effect on osteoblasts' development, accelerate the healing process and avoid undesirable outcomes such as fibrous encapsulation and bacterial infection [13-14]. A solid example of the favorable effects of surface treatments on osteointegration of biomaterials surfaces is the functionalization by grafting of bioactive polymers such as poly(sodium styrene sulfonate) (PNaSS). This method has drawn attention lately as a simple, cheap, and safe way to improve cell adhesion and development on different surfaces [15-17]. In a matter of fact, the grafted surfaces are capable of modifying the conformation of the extracellular protein, exposing active binding sites for integrin and bone growth factors [18]. This mechanism stimulates early osteoblast attachment [19], which can later escalate to generate higher calcium deposition [19-21] and bone formation

[22-23]. Besides, previous studies have shown a preventive effect of sulfonated groups on bacterial adhesion [24-27], meaning that the PNaSS grafting could act on both osteoinductive and bactericide front. The goal of this article was to graft harmonic TiNbZr surfaces with PNaSS aiming to improve the cell response of an alloy with known favorable bulk properties. The results confirmed the successful grafting of the alloy as well as the superior cell attachment and mineralization over grafted surfaces.

## 2. Materials and methods

### 2.1 Materials

The hereafter called TiNbZr alloy (chemical composition as follows (wt%) Nb = 25.22, Zr = 24.92, Fe = 0.08, C = 0.03, N = 0.01, H = 0.01, O = 0.08, Ti =49.65) was fabricated by Plasma Rotating Electrode Process (PREP) as previously described [27]. Briefly, the powder formed was milled in a planetary ball mill apparatus (SUJ2; 5 mm balls; rotation speed: 150 rpm; Ar atmosphere; RT; Ball-to-powder ration: 9:2) and the obtained bimodal powder was sintered by Spark Plasma Sintering (SPS) under the pressure of 100 MPa at 1073K for 30 min. The resulting harmonic structure consists of a three-dimensional ultra-fine grain shell surrounding a coarse-grained core. [28] Figure 1 shows a TiNbZr harmonic structures. It is observed that the sample prepared from ball milled power presents the so-called harmonic structure design consisting of ultrafine-grained skeleton and multi-crystalline equiaxed lamellar core. [29]

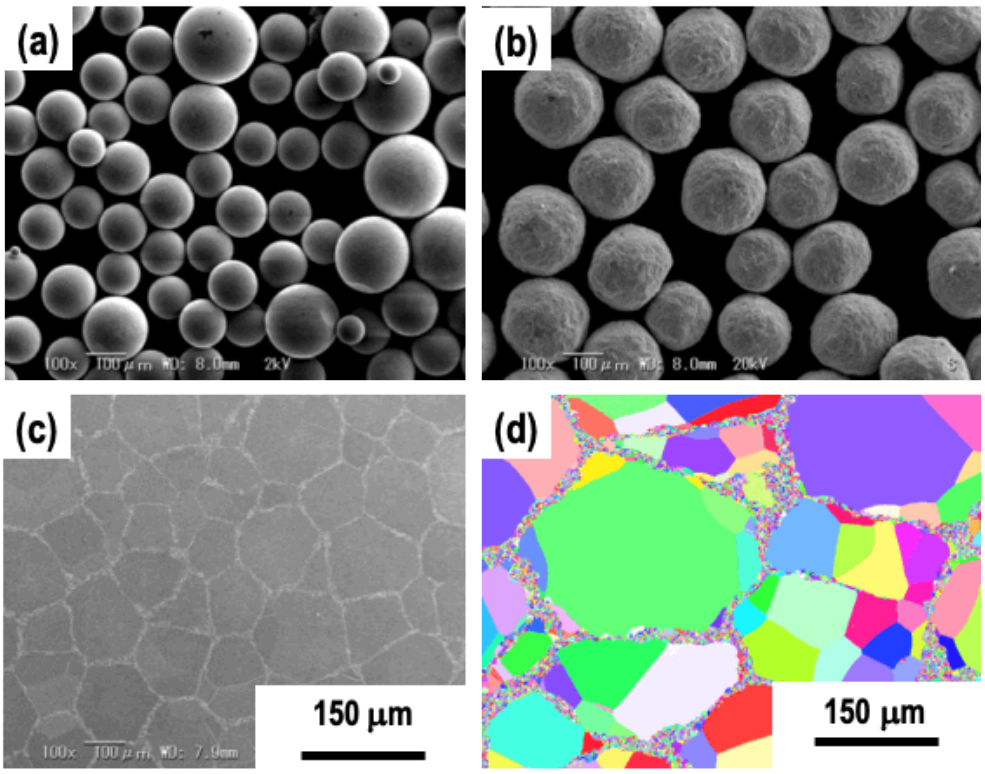


**Figure 1:** SEM images showing the designed harmonic structures of TiNBZr [29] (a): SEM image of the starting pre-alloyed powder; (b): SEM image of the powder after controlled ball milling (BM); (c): SEM image showing the bulk harmonic-structured alloy after SPS consolidation of the BMed powder; (d): Inverse pole figure (IPF) image via EBSD analysis of (c) illustrating a random crystallographic texture of the processed alloy

The TiNbZr alloy was EDM-machined to create discs. Commercially pure titanium (Ti-cp, grade 2, Goodfellow) was used as a control group for this study. TiNbZr and Ti-cp samples were polished (both faces) with SiC grinding papers (500 and 1200 consecutively). After polishing, the surfaces were successively cleaned in acetone (Fisher Scientific) bath for 15 min and in cyclohexane (Fisher Scientific), isopropanol (Sigma Aldrich), and distilled water ($dH_2O$) baths for 5 min, all under sonication.

Sodium styrene sulfonate (NaSS, Sigma) was purified before used by recrystallization in a mixture of water/ethanol (10:90 v/v) [15]. The purified NaSS was then dried under atmospheric pressure at 50°C overnight and then stored at 4°C.

### 2.2 Grafting of polyNaSS onto Ti alloys' surfaces

Firstly, TiNbZr and Ti-cp discs (14 mm) were put in Kroll's reagent (2% HF, Sigma; 10% $HNO_3$, Acros, and 88% $dH_2O$) for one minute under stirring followed by five consecutive distilled water baths, 15 minutes each, under sonication. After, the surfaces were oxidized by immersion in sodium hydroxide solution (1M) for 1 h under stirring at 80°C, followed by distilled water bath at 80°C during 1h. Following the oxidation, the surfaces were immersed into a round bottom flask containing NaSS aqueous solution (0.35 M) and irradiated with UV light (365 nm for Lotoriel UV lamp, Lot Quantum Design, emission power of up to 160 $mW/cm^2$, arc light source) at ambient temperature under stirring for 1 hour. The grafted surfaces were then washed for 48 h with distilled water and dried overnight at 37 °C before characterization.

### 2.3 Surface characterization

After each surface modification step, TiNbZr samples were characterized by toluidine blue colorimetric assay, Water contact angle measurement (WCA), Fourier-transform infrared spectra recorded in attenuated total reflection mode (ATR-FTIR), Scanning electron microscopy (SEM), and X-ray photoelectron spectroscopy (XPS) to survey changes in terms of surface compositions, physical properties or surface textures.

#### 2.3.1 Toluidine blue colorimetric method.

Toluidine Blue (TB) (CARL ROTH) is used to quantify the concentration of polymer grafted on samples. 3 samples were used for each grafting were analyzed. The grafted disks were immersed in 5 mL of TB solution (5 X $10^{-4}$ M, pH=10) at 30 °C for 6 h to allow complexation of TB with the anionic groups of the grafted polymers on surfaces. It is assumed that 1 mol of toluidine blue forms a complex with 1 mol of sulfonate group [30]. Non-complexed TB molecules were removed by 3 washing in a solution of sodium hydroxide (1 X $10^{-3}$ M). Finally, decomplexation of the TB was done by immersion in 10 mL of acetic acid/ distilled water (50: 50 v/v) for 24 h at room temperature. The concentration of decomplexed TB was measured by visible spectroscopy (Perkin Elmer, lambda 25 spectrometer) at 633 nm. Ungrafted samples were used as controls of non-specific absorption.

### 2.3.2 Water Contact Angle measurements (WCA)

The surface wettability was determined by the water contact angles, measured using a DSA10 contact angle measuring system (KRUSS GmbH) under ambient conditions. A droplet was deposed over the samples from the tip of a microliter syringe supported above the sample stage. The image of the droplet was captured and the contact angle was measured using the DSA drop shape analysis program from KRUSS. The contact angle of $dH_2O$ (2µL) on the surface was recorded 10 seconds after contact, 3 measurements were taken and averaged.

### 2.3.3 Analyses by Fourier-transform infrared spectra recorded in attenuated total reflection mode (ATR FT-IR)

The Fourier-transformed infrared (FT-IR) spectra, recorded in an attenuated total reflection (ATR), were obtained using a Perkin Elmer Spectrum Two Spectrometer equipped with a diamond crystal of 4 $cm^{-1}$ resolution. The disks were uniformly pressed against the crystal and for each surface, 128 scans were acquired (4000–500 $cm^{-1}$).

### 2.3.4 Scanning electron microscopy (SEM) analyses

The surface micro-topography of the grafted surface disks was analyzed by scanning electron microscopy (SEM, Hitachi TM3000). No further sample preparation was used before images.

### 2.3.5 X-ray photoelectron spectroscopy (XPS)

To examine possible change in terms of surface elementary composition after the functionalization, the presence of sulfur atoms attributed to PNaSS grafting TiNbZr was investigated by XPS. These analyses were performed using an Omicron Argus spectrometer (Taunusstein, Germany) equipped with a monochromated $AlK_\alpha$ radiation source ($h\nu$ = 1486.6 eV) working at an electron beam power of 300 W. Photoelectrons emission was analyzed at a takeoff angle of 90°; the analyses were carried out under ultra-high vacuum conditions ($\leq 10^{-10}$ Torr) after introduction via a load lock into the main chamber. Spectra were obtained by setting up a 100 eV pass energy for the survey spectrum and a pass energy of 20 eV was chosen for the high-resolution regions. Binding energies were calibrated against the C1s binding energy of aliphatic carbon atoms

at 284.8 eV. Element peak intensities were corrected by Scofiel factors [31] Casa XPS v.2.3.15 software (Casa Software Ltd, UK) was utilized to fit the spectra and Gaussian/Lorentzian ration was applied (G/L ration = 70/30).

Using the following formula, it was possible to determine the thickness of the grafting:

$$\frac{I}{I0} = \exp(-\frac{d}{\lambda cos\theta})$$

Where $\theta = 90°$, $I_0$=23184 cps, $I_{PNaSS}$=12640 and l = 28.1 Å

Inelastic electron mean free paths were calculated from the Tanuma, Powell and Penn TPP-2M formula using QUASES-IMFP-TPP2M Ver. 3.0 software. [32]

**2.4 Evaluation of cell viability, morphology, and mineralization**

Preceding the cell culture, grafted, non-grafted, and control samples were cleaned by successive washes in saline solutions (NaCl 1.5 M for 3x3 hours, NaCl 0.15 M for 3x3 hours, and PBS for 3x3 hours) and sterilized in ethanol (70% v/v solution) for 20 minutes and UV irradiation (underflow hood) for 15 minutes each side. Finally, the samples were conditioned by immersion in culture alpha-MEM media for 24 hours and by immersion in complete alpha-MEM media (1% penicillin, 1% glutamine, 10% fetal bovine serum) overnight at 37°C. The cell culture assays were performed under flow hood in sterile conditions using pre-osteoblast cells line MC3T3-E1 (passage 3-6).

The cell viability was assessed by MTT assay (3- (4,5-dimethyl thiazolyl-2) - 2,5-diphenyltetrazolium bromide, Sigma-Aldrich). The samples were transferred to a well plate and incubated (37 °C, 5% $CO_2$) with 250 µl of cell suspension (100.000 cells/ml). The cell suspension was also added to wells without samples as a positive control. After 24 hours the wells were empty, rinsed twice and PBS and 250 µl of MTT solution (1mg/ml, in phenol-red-free culture media) were deposed over the cells. The MTT solution was likewise added to wells without cells as a negative control. After 4 hours of incubation at 37 °C, the wells were empty, rinsed in PBS, and the formazan crystals formed by cell activity dissolved using 100 µl of DMSO

for 10 minutes under stirring. The light absorbance of the resulting solutions was read at 570 nm (MP96 SAFAS plate reader). The survival rate was calculated using the following equation:

$$SR = \frac{(\mathrm{ODs} - \mathrm{ODb})}{(\mathrm{ODc} - \mathrm{ODb})} \times 100$$

Where ODs stands for the light absorbance of the samples, ODc the light absorbance of the positive control, and ODb the light absorbance of the negative control.

The cell distribution over the samples was evaluated after 1, 4 and 24 hours in contact with TiNbZr grafted, non-grafted, and Ti-cp control samples, using the same culture conditions of viability assay. For each time point, the samples were rinsed twice in PBS and the cells were fixed in formaldehyde (4% v/v in PBS) for 30 minutes at room temperature. The cell observation was done using environmental scanning electron microscopy (ESEM - Hitachi TM3000), the instrument operated at 5 kV to 15 kV.

The differentiation of the MC3T3-E1 cells was assessed by alkaline phosphatase activity (ALP) and calcium deposition. For both essays, the cells were cultured using an osteogenic medium (complete alpha-MEM + 0.05 mM L-ascorbic acid and 10 mM beta-glycerophosphate) using 1 ml of cell suspension (50.000 cell/ml).

ALP was evaluated for 7 and 14 days of cell culture. After the time point was reached the samples were rinsed twice in PBS, transferred to a new well, and immersed in 1 ml of triz-triton x100 buffer solution for 1 hour. The suspensions were collected and vortexed before 3 cycles of freezing at -80°C and thawing at 37°C. 500 µl of the resulting suspension was mixed to 500 µl of a 20 mM solution of p-nitrophenyl phosphate and kept at 37°C for 30 min. The p-nitrophenol produced was measured by UV-vis spectrophotometry (405 nm, PerkinElmer Lambda 25). The results were normalized to the total protein amount on the sample (Pierce Rapid Gold BCA Protein Assay Kit, Thermo Scientific, France).

Calcium deposition was assessed by Alizarin red S staining assay after 14 and 28 days of culture. Before staining, the samples were rinsed twice with PBS and fixed in 4% formaldehyde for 30 min at room temperature. Following, the samples were immersed in 1 ml of Alizarin red S solution (40 mM) for one

hour. After washing with distilled water the stained samples were immersed for 15 min in a cetylpyridinium chloride solution (10 mM). Using the standard curve of Alizarin red S staining concentrations, the absorbance (560 nm, Perkin Elmer Lambda 25 spectrometer) of the decomplexed solutions can be correlated to the calcium amount on the samples. 1 M of staining is assumed to complexes 2 M of calcium [23].

### 2.5 Statistical Analyses

All values are represented by mean ± standard deviation. 3 samples were used per condition. Statistical significance was determined by one-way analysis of variance (ANOVA, p= 0.05, p = 0.01 for biological evaluation)

## 1. Results:

### 3.1 Grafting of PNaSS onto titanium alloys

In order to improve the biological response onto TiNbZr surfaces, we have decided to associate chemical modification by the grafting of bioactive polymers and the microstructure modification. So, TiNbZr alloys were oxidized in basic conditions by using sodium hydroxide solution (1M) to form hydroxide species on the surfaces. Then, exposed to 60 min of UV irradiation (160 mW/cm$^2$) to grafting (as the scheme of figure 2).

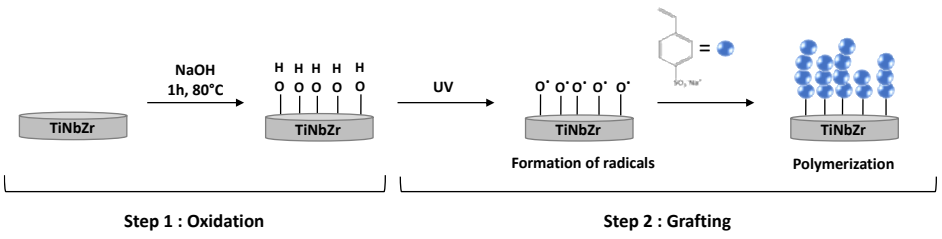


**Figure 2:** Two-steps mechanism of grafting polyNaSS on TiNbZr surface**.**

The results showed similar grafting rate of PNaSS onto these new titanium alloys and (4,52 ± 0,35 µg/cm$^2$) and Ti-cp (4,45 ± 0,07 µg/cm$^2$) (Figure 2A). The average values were close to previously verified for Ti-cp surfaces grafted by UV irradiation [33-34]. Ungrafted alloys and Ti-cp samples were used as controls and no non-specific TB absorption was verified.

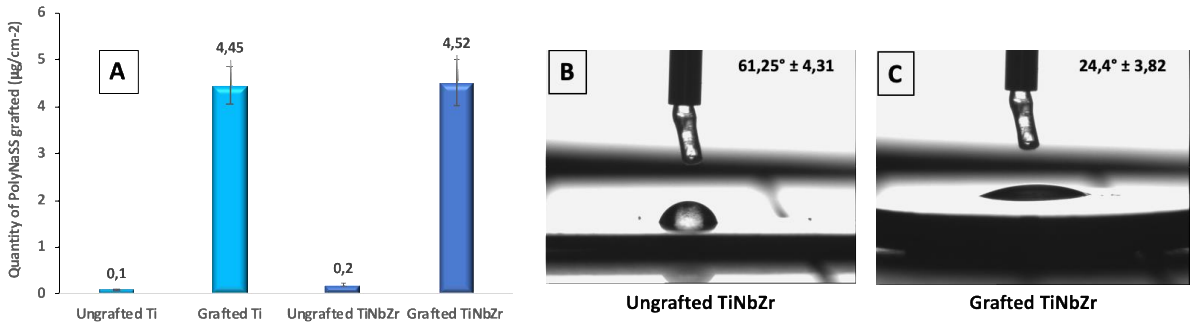


**Figure 3:** A) UV Grafting of polyNaSS at 160 mW/cm$^2$ onto Ti-cp and TiNbZr surfaces, B) WCA of ungrafted TiNbZr surface, WCA of grafted TiNbZr surface ($p < 0.05$)

On Figure 3, the water contact angle of grafted TiNbZr surfaces presented an average contact angle of 24,4° against 61,25° of polished TiNbZr samples, suggesting the presence of PNaSS, (known to be a hydrophilic polymer) [33-35]. The ATR FT-IR spectra conducted over UV grafted TiNbZr showed the presence of specific peaks of the PNaSS. Figure 4 shows the spectra of titanium alloy surface ungrafted and grafted with PolyNaSS between 900 and 1700 cm$^{-1}$.

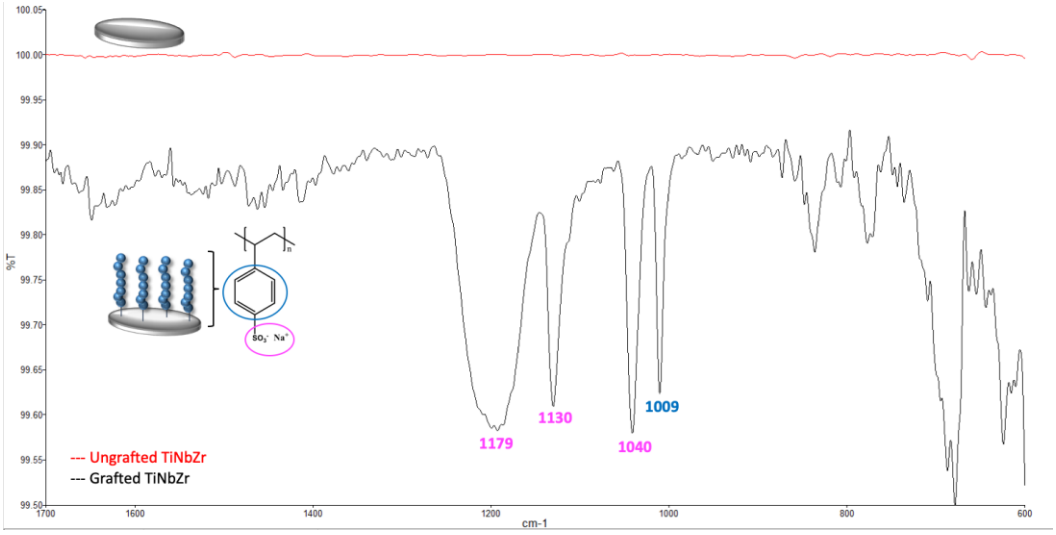

**Figure 4:** FTIR-ATR spectra of ungrafted TiNbZr surface (in red) and grafted TiNbZr surface (in black)

While no meaningful peak was observed for ungrafted TiNbZr, several peaks confirm the presence of the polymer on the grafted surface, such as the aromatic ring and the symmetric vibrations of the $SO_3^-$ groups generating a NaSS doublet (O=S=O) located at 1013 and 1040 $cm^{-1}$. Besides, the absorption of the sulfonate was detected by the peaks between 1132 and 1184 $cm^{-1}$, which is also associated with asymmetric vibrations. This same kind of interaction was found for the group $SO_2$ at 1411 $cm^{-1}$ and finally, the series of peaks between 1636 and 1450 $cm^{-1}$ is attributed to stretching vibrations of bonds (C=C) of the benzene ring (Table 1). Table 1 summarizes the peaks identified and corresponding bonds.

Table 1: adsorption bands characteristic of polyNaSS [33-34].

| **Wavelength($cm^1$)** | **Peak intensity** | **Chemical groups & interactions** |
|---|---|---|
| 1636-1450 | Low | ν(C=C) from the aromatic ring |
| 1409 | Medium | ν($SO_2$) |
| 1184-1132 | High | $SO_3^-$ (Salt) |
| 1040 | High | ν(O=S=O) |
| 1013 | High | Aromatic ring |

XPS analyses were also performed on the ungrafted and grafted TiNbZr surfaces. The survey spectrum showed the presence of the characteristic atoms of the TiNbZr (Figure 5), as well as the expected presence of oxygen and carbon, at 531 and 285 eV, respectively. The spectrum of grafted TiNbZr shows the additional presence S2p at 174 eV (together with the S2s peak at around 230 eV), reaffirming the successful grafting of PNaSS onto alloy surfaces. Quantitative analyses show the presence of titanium, Niobium,

Zirconium, Carbon, Oxygen and sulfur, and also confirm TiNbZr composition (Table 2). Additionally, for grafted surfaces the XPS analysis permitted to estimate an equivalent homogeneous thickness of the grafting of 17.1 Å, representing 3.9% (atomic ratio) of the extreme surface composition. Similar amounts of sulfur were previously found in thermally grafted titanium [31; 36].

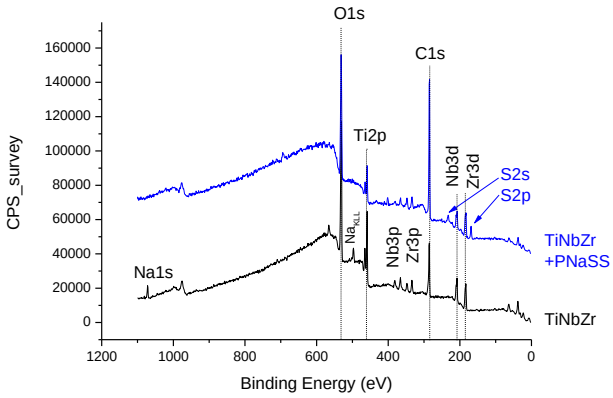


**Figure 5: XPS survey spectra of ungrafted and grafted TiNbZr**

**Table 2:** Elementary composition in atomic percentage obtained from XPS analysis of ungrafted and grafted surfaces.

| TiNbZr | Ti2p | Nb3d | Zr3d | C1s | O1s | 2S2 |
|---|---|---|---|---|---|---|
| **Ungrafted** | 9.3 | 3.0 | 3.8 | 41.3 | 42.6 | -- |
| **Grafted TiNbZr** | 3.1 | 1.5 | 2.5 | 63.0 | 26.0 | **3.9** |

### 3.2. Cellular response

The cell viability was estimated by the mitochondrial activity of the MC3T3-E1, which reduces the MTT salt into formazan crystals. The presence of formazan over grafted and non-grafted was normalized by standard polystyrene well plates. Figure 6 shows the percentage of viable cells for both groups.

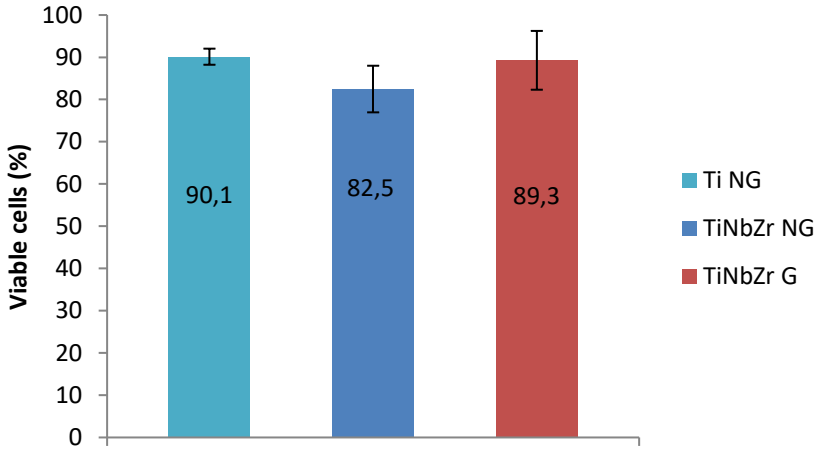


**Figure 6:** Percentage of viable MC3T3-E1 cells over non-grafted Ti, grafted, and non-grafted TiNbZr samples after 24 hours of cell culture.

Both studied groups have no sign of cytotoxicity with more than 80% of viable cells. Even if no statistical difference was observed between the groups ($p=0.01$) the mean value of viable cells over grafted samples was superior to the value for the non-grafted group, with almost 90% of active cells.

Such effect was also confirmed by the scanning electron microscopy images, as seen in figure 7. At the first observation time point (2 hours of cell culture) no significant difference was noticed on the presence of the cells over grafted and non-grafted surface, however after 4 hours of culture, the grafted surfaces starting to take the lead while a small evolution was detected for non-grafted samples. Finally, after 24 hours, the grafted surface was extensively recovered with a cell network, way denser than the non-grafted group, which had still plenty of space until confluence. This behavior is very similar to the already observed in surfaces grafted by PNaSS and can be explained by the conformation of adsorbed proteins in the presence of the polymer, which will expose sites favorable to integrin binding and, consequently cells attachment [36; 37].

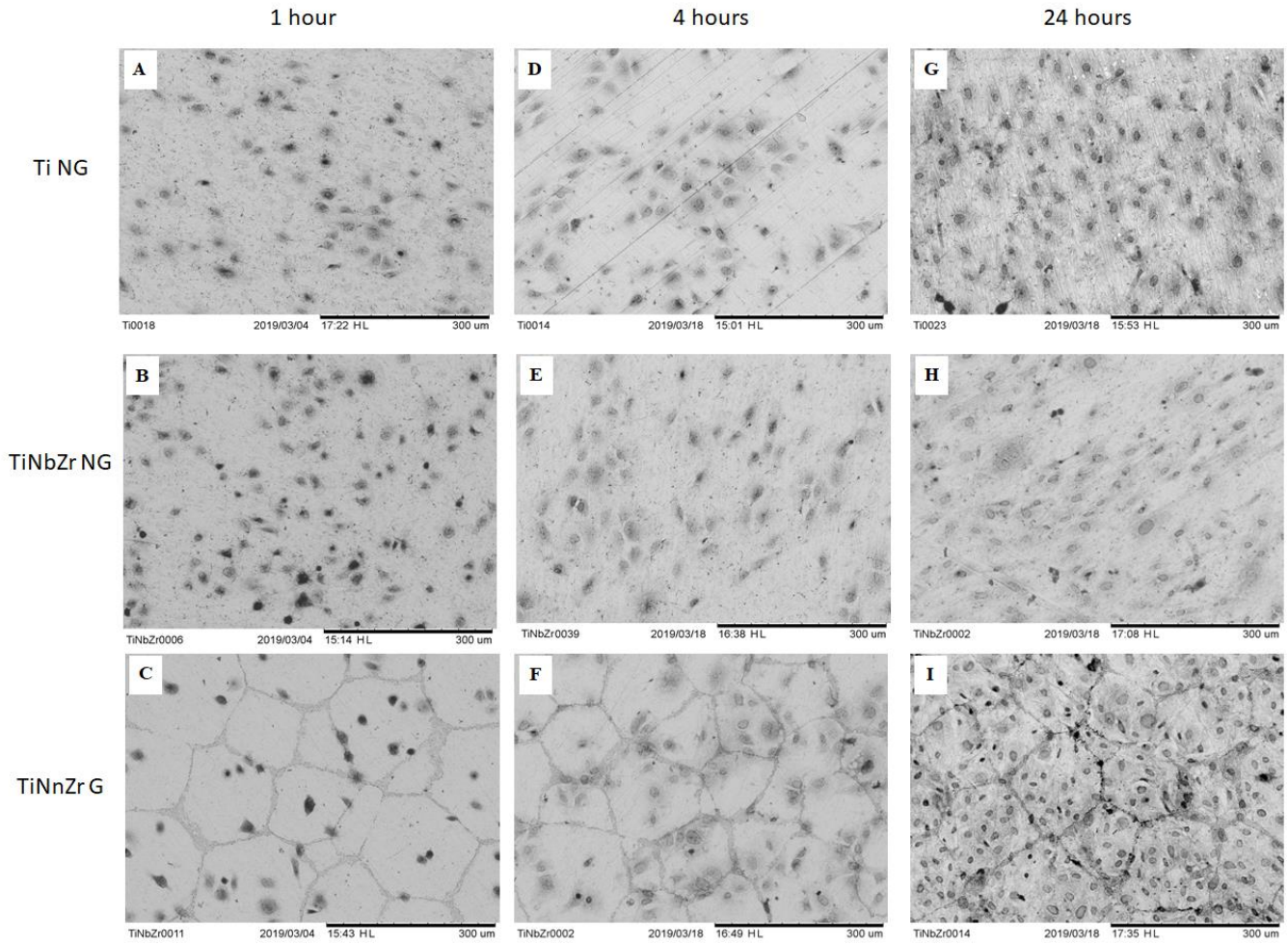


**Figure 7.** Scanning Electron Microscopy images of MC3T3-E1 pre-osteoblast cells after 1 hour over A) Ti samples, B) Non-grafted TiNbZr samples, C) Grafted TiNbZr samples; 4 hours over D) Ti samples, E) Non-grafted TiNbZr samples, F) Grafted TiNbZr samples; and 24 hours over G) Ti samples, H) Non-grafted TiNbZr samples, I) Grafted TiNbZr samples.

The evaluation of cell differentiation towards new bone cells was divided in two steps. Initially, ALP activity was assessed after 7 and 14 days of culture. The results showed in figure 7 indicate a neat advantage of enzymatic activity on grafted samples after 7 days of culture.

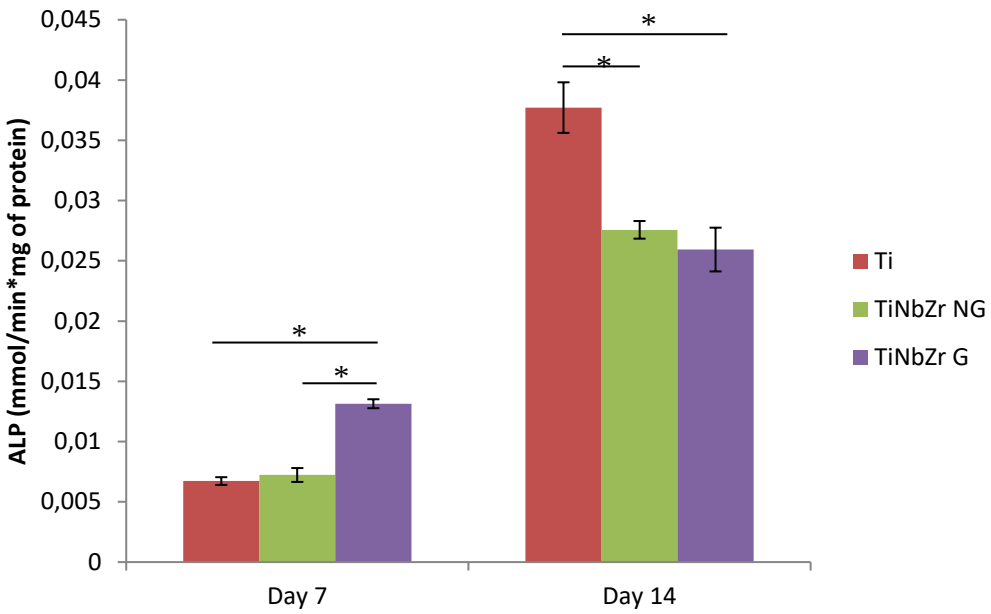


**Figure 8.** Alkaline phosphatase activity of MC3T3-E1 pre-osteoblasts over Ti control samples, Non-grafted TiNbZr samples and Grafted TiNbZr samples after 7 and 14 days of culture (*p-value < 0.05%)

The second step of cell differentiation is the formation of mineralized bone cells by apparition of calcium nodules. Calcium content After 14 and 28 days is significantly higher on grafted TiNbZr compared to Ti-cp and ungrafted TiNbZr (Figure 9). These results show that the TiNbZr structure and the grafting by PNaSS stimulates mineralized of the matrix.

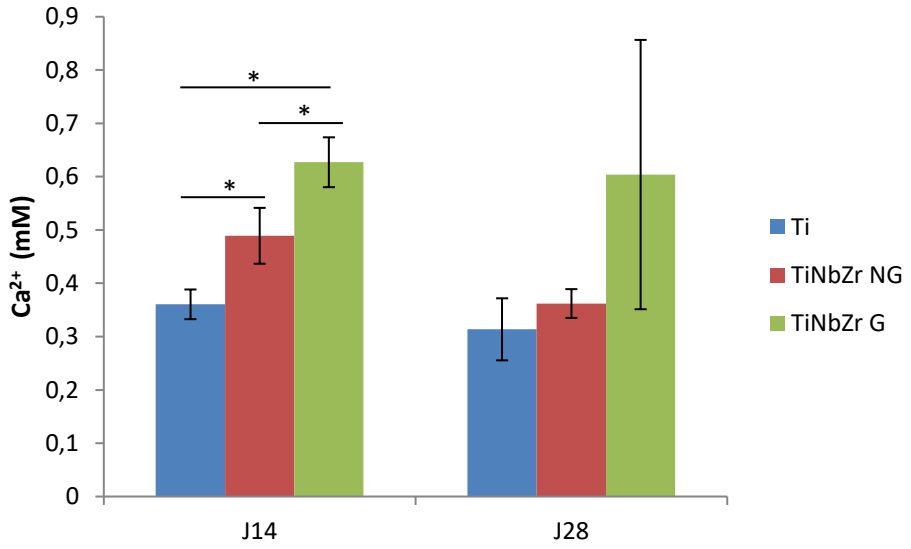

**Figure 9.** Calcium deposition measured by alizarin red method over Ti samples, Non-grafted TiNbZr samples and Grafted TiNbZr samples after 14 and 28 days of culture.

## 4. Discussion

Materials for developing bone implants like dental implants or hip prostheses must present umber advantages: high mechanical strength, corrosion resistance, a low elasticity modulus and good biocompatibility [33-34]. Titanium and its alloys are largely used for various biomedical applications. They largely replaced the Chrome-Cobalt alloys which posing serious problems of biocompatibility and the steel, which presented a young modulus too distant from that the human bone. So, titanium and its alloys have many advantages such as an excellent corrosion resistance in particular completely to the body fluids and they are the most biocompatible metals. One of the reasons why good attachment of implant materials to bone tissue remains a problem is the elastic modulus shift between the biomaterials and the surrounding bones. To ensure real integrity of the implant and maintain a real load distribution between the implant and the bone, it's imperative that the biomaterial has a module of elasticity as close as possible to that of the bone (30-50 GPa against 110 GPa for titanium).

TiNbZr alloys have been drawing great attention in recent years for biomedical applications due to their appealing mechanical properties especially for its low elastic modulus (50-80 GPa) and its fair biocompatibility. In this context, we have decided to develop the grafting of bioactive polymers bearing sulfonate groups on TiNbZr surfaces to improve their biocompatibility and osteoblast functions pertinent to new bone formation. The objective of this study is to associate chemical modification by the grafting of bioactive polymers and the microstructure modification. The first part of our study consisted of the development of the grafting onto TiNbZr surfaces. Previous studies carried out in our laboratory have shown that the grafting of bioactive polymers such as poly(styrene sulfonate of sodium) onto titanium and Ti alloy surfaces can favor osteoblast cell adhesion and differentiation [23; 27].

Basic oxidation of TiNbZr surfaces creates titanium hydroxides at the surface, which under UV irradiation produce radicals to initiate the polymerization of ionic monomer NaSS (Figure 2). The results have shown efficiency to covalently graft bioactive polymers onto TiNbZr surfaces. In this study, UV irradiation (160 $mW/cm^{-2}$) was used to induce decomposition of TiNbZr hydroxides to radicals to initiate the polymerization of aqueous solution of monomer (NaSS) in which oxidized titanium alloy samples were immersed. Using a range of different techniques to measure the presence of bioactive polymers at the TiNbZr surfaces, this study has shown a grafting rate of $4{,}52 \pm 0{,}35\ \mu g/cm^2$ with 0,35 M of monomer concentration, with a power lamp of 160 $mW/cm^{-2}$ (Figure 3) and an UV exposure of 1 h. Compared with our past study onto titanium surfaces, we obtain similar results [21, 33-34]. Moreover, XPS, ATR FT-IR analysis and the reduction of WCA have confirmed the presence of the bioactive polymer at the surface (Figure 3-5).

In parallel, the biological response study was carried out: cells viability is part of the cytotoxicity test required regarding the evaluation of biomaterial devices. Standards state to 70% the limit above which a material is qualified as non-cytotoxic [37]. MTT test used to assess cellular metabolic activities have shown that ungrafted TiNbZr and grafted TiNbZr were higher than 70% (Figure 6). These results confirm the non-cytotoxicity of the TiNbZr surfaces and the presence of the bioactive polymer.

Qualitatively, osteoblasts' shape, spreading and morphology of interesting indicators to observe surface suitability (Figure 7). After 2 hours of cell culture, no significant difference was noticed in the presence of the cells over grafted and non-grafted surface. But after 24 hours, we can observe a better evolution of the cell recovery on the grafted surface than the un-grafted surface. These results are similar to those previously found for PNaSS grafted surfaces [19] and can be explained by the conformation of adsorbed proteins in the presence of the PNaSS, which will expose sites favorable to integrin binding and, consequently cells' attachment [38; 39].

The ALP activity was reported to catalyze the formation of calcium orthophosphates, such as hydroxyapatite [40]. Thus, it is one of the first indications of calcification and it is expected to take place at an early stage of the process [41]. This feature could explain why after 14 days the ALP seems to have

reached a plateau on harmonic surfaces while the non-grated titanium is still rising (Figure 8). The profile of the ALP verified on the studied samples could indicate an acceleration of the mineralization process due to the presence of PNaSS. To confirm this phenomenon, previously verified in grafted Ti [15], the deposition of $Ca^{2+}$ was evaluated by alizarin red staining (Figure 9). The results ratify the initial hypotheses of early maturation of MC3E3-E1 cells, showing statistically superior calcium deposition over grafted samples after 14 days of culture when compared to non-grafted titanium control and alloy. More interesting, a slight reduction of calcium levels was verified for non-grafted samples after 28 days while the average values remain the quite stable for the grafted ones, resulting in a more important gap between the calcium content over the surfaces with and without PNaSS grafting (22% more calcium after 14 days and 40% more after 28 days).

This study indicates that (1) sulfonate groups grafted onto TiNbZr surfaces did not have any toxic effects on osteoblasts and (2) promoted expression of bone cell differentiation markers such as ALP activity and mineral formation. These results are similar to those previously found for PNaSS grafted surfaces [19] and endorse the positive effect of the PNaSS on cell/material interaction.

## Conclusion

Our purpose was to apply the methods used previously in the laboratory in terms of bioactive polymers grafting in particular by UV irradiation onto the surface of newly developed titanium alloys TiNbZr. UV irradiation was used to induce decomposition of titanium hydroxides to radicals to initiate the polymerization of an aqueous solution of monomer (NaSS) in which oxidized titanium alloy samples were immersed. Using various techniques to measure the presence of bioactive polymers onto the surface, this study has shown that our rates of grafting obtained on these new alloys are as good as (around 4,5 $\mu g/cm^2$) as those of grafting on classical alloys. In parallel, *in vitro* biological response study was carried out to assess toxicity, cell viability, and morphology on the titanium alloys TiNbZr functionalized or not by bioactive polymers giving encouraging results. Moreover, results showed superior alkaline phosphatase

activity and higher calcium deposition on grafted samples, implying a beneficial effect of the PNaSS in osteoinduction activity.

**Acknowledgments**

Part of this work was supported by the Japan Society for the Promotion of Science (JSPS) Grant Numbers 18K18962 and JP18H05256. This research was supported by the French Ministry of National Education, Higher Education, and Research. The authors thank IMPC (Institut des Matériaux de Paris Centre, FR2482) and the C'Nano project of Region Ile-de-France, for Omicron XPS apparatus funding.

**Credit Authorship statement**

A. RANGEL: Biological analysis, Visualization, Writing; A. HOCINI: EBSD analysis; V. HUMBLOT: Investigation, Formal analysis, Editing; K. AMEYAMA: Concept and Materials processing; V. MIGONNEY: Resources; G. DIRRAS: Materials processing, Resources, Editing; C. FALENTIN-DAUDRE: Conceptualization, Methodology, Validation, Formal analysis, Resources, Supervision, Writing - Review & Editing.

**Declaration of competing interest**

The authors declare that they have no known competing financial or personal relationships that could be viewed as influencing the work reported in this paper.

## References


[1] Pane J, Verhamme KMC, Rebollo I, Sturkenboom MCJM. Descriptive analysis of postmarket surveillance data for hip implant. Pharmacoepidemiol Drug Saf. 2020;29:380– 387. https://doi.org/10.1002/pds.4971

[2] Eger M, Sterer N, Liron T, Kohavi D, Gabet Y. Scaling of titanium implants entrains inflammation-induced osteolysis. Scientific Reports 2017;7: 39612. https://doi.org/10.1038/srep39612

[3] Lee J, Ogawa T. The Biological Aging of Titanium Implants. Implant Dentistry 2012; 21(5): 415–421. https://doi.org/10.1097/ID.0b013e31826a51f4

[4] Eisenbarth E, Velten D, Müller M, Thull R, BremeJ. Biocompatibility of β-stabilizing elements of titanium alloys. Biomaterials 2004;25(26):5705-5713. https://doi.org/10.1016/j.biomaterials.2004.01.021

[5] Meng Q, Guo S, Liu Q, Hu L, Zhao X. A β-type TiNbZr alloy with low modulus and high strength for biomedical applications. Progress in Natural Science: Materials International 2014;24 (2):157-162. https://doi.org/10.1016/j.pnsc.2014.03.007

[6] Ribeiro AL, Hammer P, Vaz LG, Rocha LA. Are new TiNbZr alloys potential substitutes of the Ti6Al4V alloy for dental applications? An electrochemical corrosion study. Biomedical Materials 2013;8(6):065005. https://doi.org/10.1088/1748-6041/8/6/065005

[7] Farbaniec L, Dirras G, Krawczynska A, Mompiou F, Couque H, Naimi F, Bernard F, Tingaud D. Powder metallurgy processing and deformation characteristics of bulk multimodal nickel. Materials Characterization 2014;94:126-137. https://doi.org/10.1016/j.matchar.2014.05.008

[8] Dirras G, Tingaud D, Csiszár G, Gubicza J, Couque H, Mompiou F. Characterization of bulk bimodal polycrystalline nickel deformed by direct impact loadings. Materials Science and Engineering A 2014;601:48-57. http://dx.doi.org/10.1016/j.msea.2014.02.043

[9] Sekiguchi T, Ono K, Fujiwara H, Ameyama K. New microstructure design for commercially pure titanium with outstanding mechanical properties by mechanical milling and hot roll sintering. Materials Transactions 2010;51(1):39-45. https://doi.org/10.2320/matertrans.MB200913

[10] Sharma B, Dirras G, Ameyama K. Harmonic Structure Design: A Strategy for Outstanding Mechanical Properties in Structural Materials. Metals 2020;10(12):1615. https://doi.org/10.3390/met10121615

[11] Vajpai1SK, Yu H, Ota M, Watanabe I, Dirras G, Ameyama K. Three-Dimensionally Gradient and Periodic Harmonic Structure for High-Performance Advanced Structural Materials. Materials Transactions 2016;57(9):1424-1432. https://doi.org/10.2320/matertrans.MH201509

[12] Wang Q, Zhou P, Liu S, Attarilar S, Ma RLW, Zhong Y, Wang L. Multi-Scale Surface Treatments of Titanium Implants for Rapid Osseointegration: A Review. Nanomaterials 2020;10(6):1244. https://doi.org/10.3390/nano10061244

[13] Spriano S, Yamaguchi S, Baino F, Ferraris S. A critical review of multifunctional titanium surfaces: New frontiers for improving osseointegration and host response, avoiding bacteria contamination, Acta Biomaterialia 2018;79:1-22. https://doi.org/10.1016/j.actbio.2018.08.013.

[14] Nicholson JW. Titanium Alloys for Dental Implants: A Review. Prosthesis 22020;2(2):100-116. https://doi.org/10.3390/prosthesis2020011

[15] Chouirfa H, Evans MDM, Castner DG, Bean P, Mercier D, Galtayries A, Falentin-Daudré C, Migonney V. Grafting of architecture controlled poly(styrene sodium sulfonate) onto titanium surfaces using bio-adhesive molecules: Surface characterization and biological properties. Biointerphases 2017;12(2):02C418. https://doi.org/10.1116/1.4985608

[16] Rangel A, Nguyen TN, Egles C, Migonney V. Different real-time degradation scenarios of functionalized poly (ε-caprolactone) for biomedical applications. Journal of Applied Polymer Science 2021;138(17):50479. https://doi.org/10.1002/app.50479

[17] Vaquette C, Viateau V, Guérard S, Anagnostou F, Manassero M, Castner DG, Migonney V. The effect of polystyrene sodium sulfonate grafting on polyethylene terephthalate artificial ligaments on in vitro mineralization and in vivo bone tissue integration. Biomaterials 2013;34(29):7048-63. https://doi.org/10.1016/j.biomaterials.2013.05.058

[18] Oughlis S, Lessim S, Changotade S, Bollotte F, Poirier F, Hélary G, Lataillade J, Migonney V, Lutomski D. Development of proteomic tools to study protein adsorption on a biomaterial, titanium grafted with poly(sodium styrene sulfonate). Journal of Chromatography B: Analytical Technologies in the Biomedical and Life Sciences 2011;879(31):3681–3687. https://doi.org/10.1016/j.jchromb.2011.10.006

[19] Rangel A, Falentin-Daudré C, Silva Pimentel BNA, Vergani CE, Migonney V, Alves Claro APR Nanostructured titanium alloy surfaces for enhanced osteoblast response: A combination of morphology and chemistry Surfaces Coatings and Technology 2020;383: 125226. https://doi.org/10.1016/j.surfcoat.2019.125226

[20] Alcheikh A, Pavon-Djavid G, Helary G, Petite H, Migonney V, Anagnostou F. PolyNaSS grafting on titanium surfaces enhances osteoblast differentiation and inhibits Staphylococcus aureus adhesion. Journal of Materials Science: Materials in Medicine 2013;24:1745–1754. https://doi.org/10.1007/s10856-013-4932-3

[21] Mayingi J, Hélary G, Noirclere F, Bacroix B, Migonney V. Synthèse et greffage de polymères bioactifs sur des surfaces en titane pour favoriser l'ostéointégration Grafting of bioactive polymers onto titanium surfaces and human osteoblasts response. ITBM-RBM 2008;29:1–6. https://doi.org/10.1016/j.rbmret.2007.10.001

[22] Kerner S, Migonney V, Pavon-Djavid G, Helary G, Sedel L, Anagnostou F. Bone tissue response to titanium implant surfaces modified with carboxylate and sulfonate groups. Journal

of Materials Science: Materials in Medicine 2010;21:707–715. https://doi.org/10.1007/s10856-009-3928-5

[23] Felgueiras H, Decambron A, Manassero M, Tulasne L, Evans M, Viateau V, Migonney V. Bone tissue response induced by bioactive polymer functionalized Ti6Al4V surfaces: In vitro and in vivo study. Journal of Colloid and Interface Science. 2017:491:44–54. https://doi.org/10.1016/j.jcis.2016.12.023

[24] Ben Aissa I, Helary G, Migonney V. Le greffage radicalaire de polymères bioactifs sur le titane pour prèvenir l'infection sur prothèse articulaire. IRBM 2011;32(5):322–325. https://doi.org/10.1016/j.irbm.2011.07.002

[25] Zhou J, Pavon-Djavid G, Anagnostou F, Migonney V. Inhibition de l'adhérence de Porphyromonas gingivalis sur la surface de titane greffé de poly(styrène sulfonate de sodium), IRBM 2007 ;28(1):42-48. https://doi.org/10.1016/j.rbmret.2007.02.003

[26] Vasconcelos D, Falentin-Daudré C, Blanquaert D, Thomas D, Granja P, Migonney V. Role of protein environment and bioactive polymer grafting in the S. epidermidis response to titanium alloy for biomedical applications. Materials Science and Engineering C. 2014;45: 176–183. https://doi.org/ 10.1016/j.msec.2014.08.054

[27] Chouirfa H, Evans MDM, Bean P, Saleh-Mghir A, Crémieux AC, Castner DG, Falentin-Daudré C, Migonney V. Grafting of Bioactive Polymers with Various Architectures: A Versatile Tool for Preparing Antibacterial Infection and Biocompatible Surfaces. ACS Applied Material Interfaces. 2018;10(2):1480-1491. https://doi.org/10.1021/acsami.7b14283

[28] Ueda D, Dirras G, Hocini A, Tingaud D, Ameyama K, Langlois P, Vrel D, Trzaska Z. Data on processing of Ti-25Nb-25Zr β-titanium alloys via powder metallurgy route: Methodology, microstructure, and mechanical properties. Data Brief 2018;18:703-708. https://doi.org/10.1016/j.dib.2018.01.093

[29] Vajpai SK, Ota M, Zhang Z, Ameyama K. Three-dimensionally gradient harmonic structure design: an integrated approach for high performance structural materials. Mater. Res. Lett. 2016 ;4(4):191–197. https://doi.org/10.1080/21663831.2016.1218965

[30] Michiardi A, Hélary G, Nguyen PCT, Gamble LJ, Anagnostou F, Castner DG, Migonney V. Bioactive polymer grafting onto titanium alloy surfaces, Acta Biomaterialia 2010;6(2):667-675. https://doi.org/10.1016/j.actbio.2009.08.043

[31] Scofield JH. Hartree-Slater Subshell Photoionization Cross-Sections at 1254 and 1487ev. J. Elec. Spectrosc. Relat. Phenom. *1976;8:129*–137. https://doi.org/10.1016/0368-2048(76)80015-1

[32] Tanuma S, Powell CJ, Penn DR. Calculation of electron inelastic mean free paths (IMFPs) VII. Reliability of the TPP-2M IMFP predictive equation Surf. Interf. Anal. 1994;21:165-176. https://doi.org/10.1002/sia.740210302

[33] Chouirfa H, Migonney V, Falentin-Daudré C. Grafting bioactive polymers onto titanium implants by UV irradiation. Royal Society of Chemistry Advances 2016;6:13766– 13771. https://doi.org/10.1039/C5RA24497H

[34] AmokraneG, Hocini A, Ameyama K, Dirras G, Migonney V, Falentin-Daudré C. Functionalization of new biocompatible titanium alloys with harmonic structure desing by UV irradiation. IRBM 2017;4(38):190-197. https://doi.org/10.1016/j.irbm.2017.06.008

[35] Oikonomou EK, Bethani A, Bokias G, Kallitsis JK. Poly(sodium styrene sulfonate)-b-poly(methyl methacrylate) diblock copolymers through direct atom transfer radical polymerization: Influence of hydrophilic–hydrophobic balance on self-organization in aqueous solution. European Polymer Journal 2011;47(4):752-761. https://doi.org/10.1016/j.eurpolymj.2010.09.034

[36] Zorn G, Baio JE, Weidner T, Migonney V, Castner DG. Characterization of poly(sodium styrene sulfonate) thin films grafted from functionalized titanium surfaces. Langmuir 2011;27: 13104-13112. https://doi.org/10.1021/la201918y

[37] Li M, Neoh KG, Xu LQ, Wang R, Kang ET, Lau T, Olszyna DP, Chiong E. Surface Modification of Silicone for Biomedical Applications Requiring Long-Term Antibacterial, Antifouling, and Hemocompatible Properties. Langmuir 2012;28:16408–16422. https://doi.org/10.1021/la303438t.

[38] Latz C, Pavon-Djavid G, Helary G, Evans M, Migonney V. Alternative intracellular signaling mechanism involved in the inhibitory biological response of functionalized PMMA-based polymers. Biomacromolecules (2003;4(3):766–771. https://doi.org/10.1021/bm025764g

[39] Felgueiras H, Migonney V. Sulfonate groups grafted on Ti6Al4V favor MC3T3-E1 cell performance in serum-free medium conditions. Materials Science and Engineering: C. 2014;39: 196-202. https://doi.org/10.1016/j.msec.2014.03.013

[40] Colaço E, Brouri D, Méthivier C, Valentin L, Oudet F, El Kirat K, Guibert C, Landoulsi J. Calcium phosphate mineralization through homogenous enzymatic catalysis: Investigation of the early stages. Journal of Colloid and Interface Science 2020;565:43-54. https://doi.org/10.1016/j.jcis.2019.12.097

[41] Vimalraj S. Alkaline phosphatase: Structure, expression and its function in bone mineralization. Gene 2020;754:144855. https://doi.org/10.1016/j.gene.2020.144855